Giant Oscillations in the Magnetoacoustic Attenuation of Bismuth

ARNOLD M. TOXEN AND SABIH TANSAL
IBM Watson Research Center, Yorktown Heights, New York
(Received 5 August 1964)

Measurements of the magnetoacoustic attenuation of bismuth at temperatures of 1.4–1.8°K in transverse magnetic fields up to 17 kG are reported. For shear waves of frequency 8–40 Mc/sec, propagated in the bisectrix direction, with the magnetic field in the binary direction, oscillations in the magnetoacoustic attenuation coefficient as large as 17 db/cm are observed. The oscillations in attenuation coefficient are approximately periodic in the reciprocal of the magnetic field with a period of 6.3×10^{-5} Oe^{-1}, a value corresponding to the smallest cyclotron mass. The data are compared with current theories and are found to be in qualitative agreement. More detailed comparison, however, indicates the need for a more sophisticated theory of the giant oscillations which takes into account the effects of finite electronic mean free path and deviations from parabolicity of the conduction bands. The data presented were obtained using a new and versatile sampling technique which involves the use of a commercial sampling oscilloscope.

I. INTRODUCTION

THE de Haas–van Alphen-like oscillations of the acoustic attenuation coefficient have been reported in bismuth,[1,2] zinc,[3] and antimony.[4] These oscillations are the acoustic analog of the de Haas–van Alphen oscillations in magnetic suceptibility or de Haas–Shubnikov oscillations in magnetoresistance. That is, in magnetic fields which are sufficiently large that the Landau level spacing is large compared to the thermal broadening at the Fermi surface, the acoustic attenuation coefficient undergoes quantum oscillations as a function of magnetic field which are periodic in the reciprocal of the magnetic-field intensity. When the electronic mean free path is very large compared to the sound wavelength, or, equivalently, when the product of phonon wave vector q and electron mean free path l is large compared to one, the oscillations in attenuation coefficient become proportionately much larger, and the maxima take on a distinctive spike-like shape. In this regime, they are referred to as "giant oscillations" of the attenuation coefficient and were theoretically predicted by Gurevich, Skobov, and Firsov.[5] The "giant oscillations" have been experimentally observed in zinc,[6] gallium,[7] and bismuth.[8] For the zinc and gallium measurements, the experiments were carried out in a longitudinal magnetic field with longitudinal sound waves; for the bismuth, with transverse sound waves and with the magnetic field nearly perpendicular to the sound propagation direction.

It is the purpose of this paper to indicate the present state of the theory of giant oscillations and to compare to this theory data obtained from ultrasonic measurements on bismuth single crystals. Anticipating our results, we shall show that the experimental results are in qualitative agreement with the theory. When the data are examined quantitatively, however, many discrepancies are noted which indicate the need for a more sophisticated theoretical model. In addition, we introduce a new method for taking the ultrasonic data which offers many advantages over existing techniques.

II. THEORETICAL DISCUSSION

As Gurevich, Skobov, and Firsov[5] have shown, the "giant oscillations" are a consequence of energy and momentum conservation in the absorption of a phonon by a free electron. Neglecting spin, the energy states of the "free" electrons in the presence of a magnetic field H are given by the expression

$$\epsilon=(n+\tfrac{1}{2})\hbar\Omega+\hbar^2k_z^2/2m^*, \tag{1}$$

where n is a positive integer, $\Omega=eH/m_cc$ is the cyclotron frequency, and k_z is the component of electron wave vector in the direction of the magnetic field, which has been assumed to be in the z direction. The quantities m_c and m^* are the cyclotron and effective masses, respectively. When a phonon of frequency ω and wave vector q is absorbed, we must satisfy the following condition:

$$(n+\tfrac{1}{2})\hbar\Omega+\hbar^2k_z^2/2m^*+\hbar\omega = (n'+\tfrac{1}{2})\hbar\Omega+\hbar^2(k_z+q_z)^2/2m^*, \tag{2}$$

where energy and momentum conservation have been assumed. Upon collecting terms and neglecting the term $\hbar^2q_z^2/2m^*$ (since $k_z\gg q_z$), one obtains

$$(n-n')\Omega+\omega=\hbar k_zq_z/m^*. \tag{3}$$

In a sufficiently large magnetic field, i.e., when $\Omega\gg\hbar k_zq_z/m^*$, Eq. (3) can be satisfied only for $n=n'$. Under these conditions,

$$\hbar k_zq_z/m^*=\omega. \tag{4}$$

[1] Darrell H. Reneker, Phys. Rev. **115**, 303 (1959).
[2] J. G. Mavroides, B. Lax, K. J. Button, and Y. Shapira, Phys. Rev. Letters **9**, 451 (1962).
[3] D. Gibbons, Phil. Mag. **6**, 445 (1961).
[4] J. B. Ketterson, Phys. Rev. **129**, 18 (1963).
[5] V. L. Gurevich, V. G. Skobov, and Yu. A. Firsov, Zh. Eksperim. i Teor. Fiz. **40**, 786 (1961) [English transl.: Soviet Phys.—JETP **13**, 552 (1961)].
[6] P. Korolyuk and T. A. Prushak, Zh. Eksperim. i Teor. Fiz. **41**, 1689 (1962) [English transl.: Soviet Phys.—JETP **14**, 1201 (1962)].
[7] Y. Shapira and B. Lax, Phys. Rev. Letters **12**, 166 (1964).
[8] Arnold M. Toxen and Sabih Tansal, Bull. Am. Phys. Soc. **9**, 264 (1964).

In the low-frequency range, in which we shall be interested, we can assume a linear dispersion relation for the phonons, so that $\omega=qu$, where u is the sound velocity. Substituting this result into Eq. (4), we obtain the result

$$k_z\equiv k_z^0=m^*uq/\hbar q_z=m^*u/\hbar\cos\theta, \tag{5}$$

where θ is the angle between the sound propagation direction and the magnetic field. We can also rewrite Eq. (5) in terms of the electron velocity,

$$v_z^0=u/\cos\theta. \tag{6}$$

It is very interesting to note that condition (6) or (5) is just equivalent to the condition that the electrons drift in phase with the sound wave. For, if the electrons are drifting parallel to the magnetic field with velocity v_z, the component of velocity in the $\hat{q}$ direction will be $v_q=v_z\cos\theta$. If now $v_z=v_z^0=u/\cos\theta$, it is clear that $v_q=u$. Thus, the only electrons which can absorb a phonon without changing Landau levels (i.e., $\Delta n=0$) and simultaneously conserve energy and momentum are those electrons drifting in phase with the phonon.

Let us now consider the significance of these results. As one can see from Eq. (1), n and k_z are quantum numbers that characterize the energy state of an electron in a magnetic field. The quantum number n can take on only integral values (or zero) and characterizes which Landau level the electron belongs to, whereas k_z varies continuously. When the magnetic field is high enough, or the phonon energy low enough, transitions between Landau levels are forbidden; hence, we arrive at the selection rule $\Delta n=n-n'=0$ for the absorption of a phonon. Under these conditions, Eq. (5) or (6) must be satisfied if a phonon is to be absorbed. That is, phonons can be absorbed only by electrons which are in a particular initial state k_z^0, determined by the magnetic field and propagation directions, and which can make a transition to a particular final state $k_z^0+q_z$. This process can take place only if the initial state is occupied and the final state empty, a condition which, in general, is not satisfied. This can be seen better by referring to Fig. 1 which is a plot of the allowed electron energies $\epsilon(n,k_z)$ as given by Eq. (1). The line marked ζ is the position of the Fermi energy. Clearly, only those states will be filled which lie below ζ, those which lie above ζ will be empty. If $\Delta n=0$, both conditions can be satisfied only for those carriers lying at the intersection of the Landau levels with ζ. If condition (5) is to be satisfied, however, this intersection must occur at $k_z=k_z^0$, or

$$\zeta=(n_i+\tfrac{1}{2})\hbar eH_i/m_cc+\hbar^2k_z^{0^2}/2m^* \tag{7}$$

must be satisfied for some integer n_i and field value H_i. As one can easily see, this is a very stringent selection rule and will be satisfied only at particular values of magnetic field. Thus, the attenuation coefficient, as a function of magnetic field, consists of a series of sharp maxima occurring at those H_i satisfying Eq. (7). However, in the regions between the maxima the attenuation coefficient is very small. Because the Fermi velocity is so much larger than the sound velocity, $v_F/u\sim1000$ in bismuth, k_z^0 is ordinarily much smaller than k_F and $\hbar^2k_z^{0^2}/2m^*$ is much smaller than ζ. Hence, there will be an n_i and H_i such that Eq. (7) is satisfied (unless the magnetic field is so large that $\hbar eH/2m_cc>\zeta$). However, when $\cos\theta<10^{-3}$, k_z^0 may exceed k_F, in which case, $\hbar^2k_z^{0^2}/2m^*>\zeta$, and Eq. (7) cannot be satisfied for any value of magnetic field. Thus, when the applied magnetic field is perpendicular to the sound propagation direction, the giant oscillations will disappear and the attenuation will decrease.

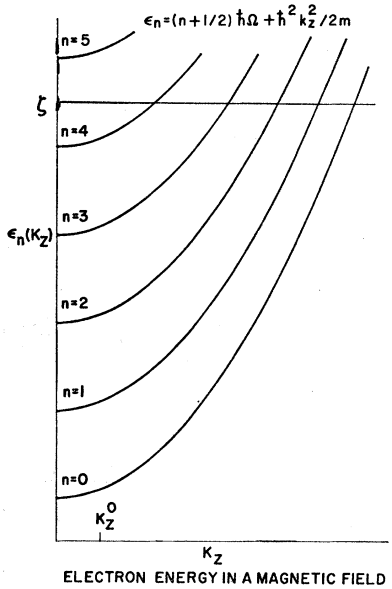

ELECTRON ENERGY IN A MAGNETIC FIELD

FIG. 1. Electronic energy levels in a quantizing magnetic field for a parabolic band. The energy $\epsilon_n(k_z)$ is a function of the quantum numbers n, which determines which harmonic oscillator level the electron occupies, and k_z, which is the component of wave vector parallel to the applied magnetic field.

Expressions for the acoustic attenuation coefficient in the "giant oscillation" region were first derived by Gurevich *et al.*[5] who treated in detail only the longitudinal case, i.e., with the sound propagation in the direction of the magnetic field. The more general case, in which the sound propagation direction is not parallel to the magnetic field and in which an electric field is present was worked out by Kazarinov and Skobov.[9] For the experimental results which will be presented, the electric field is zero and the results simplify to

$$\Gamma=\Gamma_0\frac{v_z^0}{s}\frac{\hbar\Omega}{4kT}\sum_{n=0}^{\infty}J_0^2(q_\perp R_n)\cosh^{-2}\xi_n, \tag{8}$$

where

$$\xi_n=|\zeta-\hbar\Omega(n+\tfrac{1}{2})-mv_z^{0^2}/2|/2kT. \tag{9}$$

The quantity Γ_0 is the attenuation coefficient in zero field; J_0 is the Bessel function of zero order; $q_\perp$ is $(q_x^2+q_y^2)^{1/2}$; and R_n is the average radius of the orbit

[9] R. F. Kazarinov and V. G. Skobov, Zh. Eksperim. i Teor. Fiz. 43, 1496 (1962) [English transl.: Soviet Phys.—JETP 16, 1057 (1963)].

in quantum state n and is equal to $[(2n+1)c\hbar/eH]^{1/2}$. At high frequencies or low magnetic fields, i.e., $q_\perp R_n > 1$, the magnitude of the Bessel function J_0 oscillates as a function of magnetic field. The resulting oscillations of the attenuation coefficient are known as "geometric" oscillations. The limit which is applicable to the results to be presented is the opposite limit $q_\perp R_n \ll 1$ which obtains at low frequencies and high magnetic fields. In this limit $J_0 \approx 1$ and the geometric oscillations vanish. In this regime, however, $\cosh^{-2}\xi_n$ oscillates as a function of magnetic field giving rise to the quantum oscillations. It is clear that the expression in Eq. (8) has the properties discussed previously in more general terms. In strong magnetic fields, i.e., $\hbar\Omega \gg kT$, the sum over n in Eq. (8) will be dominated by that term $n=N$ for which ξ_N is a minimum. In fact, Γ will be a maximum when $\xi_N = 0$. This is exactly condition (7), previously discussed. The resulting expression for the values of Γ at its maxima is then given by

$$\Gamma_{\max} \cong \Gamma_0 (v_z^0/s)(\hbar\Omega_{\max}/4kT), \tag{10}$$

where $\Omega_{\max}$ is the value of Ω calculated from the magnetic field at which the particular maximum occurs. The minima in attenuation coefficient will be

$$\Gamma_{\min} \cong \Gamma_0 \frac{v_z^0}{s} \frac{\hbar\Omega_{\min}}{4kT} \cosh^{-2}\frac{\hbar\Omega_{\min}}{4kT}, \tag{11}$$

where $\Omega_{\min}$ is the value of Ω calculated from the magnetic field at which the particular minimum occurs. In this limit, Γ will be periodic in the reciprocal of the magnetic field with the period given by the expression

$$\Delta(1/H) = e\hbar/m_c c(\zeta - m^* v_z^{0^2}/2). \tag{12}$$

So long as $m^* v_z^{0^2}/2$ is small compared to ζ, the period of the oscillations in Γ is the same as that of the de Haas–Shubnikov effect. However, when $m^* v_z^{0^2}/2$ becomes comparable to ζ, as when the angle between the propagation direction and magnetic field is nearly 90°, the period of the giant oscillations gets larger than that of the de Haas–Shubnikov effect. When $mv_z^{0^2}/2$ gets still larger, ξ_N cannot vanish for any value of magnetic field, and the attenuation coefficient goes to zero as $\cosh^{-2}\xi_N$.

In the discussion thus far, one important factor has been omitted; defect scattering of the electrons. In the derivation of selection rule (5), it was assumed that momentum was conserved in the electron-phonon interaction. This must be true only in the long mean-free-path limit, $ql \gg 1$. In the presence of scattering, acoustic absorption can occur simultaneously with defect scattering of the electron. In the latter case, the defect serves to supply or take up the necessary momentum. In other words, the electron momentum is not a good quantum in the presence of scattering. Thus, the effects of scattering are twofold. Firstly, the maxima in the attenuation coefficient are broadened. Secondly, even when Eq. (7) is not satisfied, there will be some phonon absorption. This contribution to the absorption is proportional to $1/ql$ and will serve to decrease the amplitude of the oscillations.

Expressions for the attenuation coefficient in the presence of scattering, i.e., for finite ql, have been obtained by Gurevich *et al.*[5] and Skobov.[10] Both treatments, however, are for the case in which the magnetic field is parallel to the sound propagation direction. Although they are not directly applicable to the experimental results to be discussed, they are of interest in that they indicate in a qualitative way the effects of defect scattering upon the giant oscillations. The treatment by Skobov appears to be rigorous, but for the case of most interest, the strong field region, i.e., $ql(\Omega/\zeta)^{1/2} \gg 1$, the result is in the form of a complicated integral to be evaluated. For the weak field case, $(\zeta/\Omega) \gg q^2 l^2 \gg 1$, Skobov obtains the result,

$$\Gamma(H) = \Gamma_0 \left\{ 1 + ql(\Omega/\zeta)^{1/2} \times \sum_{n=1}^{\infty} (-1)^n A_n \frac{\cos(2\pi n\zeta/\Omega - \pi/4)}{\pi (n)^{1/2}} \right\}, \tag{13}$$

where

$$A_n = \frac{2\pi^2 nkT/\Omega}{\sinh(2\pi^2 nkT/\Omega)}. \tag{14}$$

This result is quite interesting because it indicates that in the weak field region where $ql(\Omega/\zeta)^{1/2} \ll 1$, the oscillations are small in magnitude compared to Γ_0. In fact, Eq. (13) is very similar to corresponding expressions for the de Haas–van Alphen effect.[11]

The treatment by Gurevich *et al.*[5] takes account of scattering by smearing out the electronic energy by $\hbar/\tau$, where τ is the electronic relaxation time. This was done in an integration which is involved in the evaluation of the matrix element for phonon absorption. In this integration, $\delta(\hbar q v_z + \hbar q^2/2m - \omega)$ is replaced by $\tau^{-1}/\pi[\tau^{-2} + (\hbar q v_z + \hbar q^2/2m - \omega)^2]$, i.e., the δ function conserving energy is replaced by a Lorentzian whose width is proportional to τ^{-1}. Gurevich *et al.* then obtain the result

$$\Gamma = \Gamma_0 \frac{\hbar\Omega}{4kT} \int dy \frac{1}{\pi} \frac{B}{1+B^2 y^2} \sum_{n=0}^{\infty} \cosh^{-2}\left(\frac{y}{2} - \xi_n\right), \tag{15}$$

where

$$B \equiv ql(kT/\zeta)^{1/2}, \tag{16}$$

and the other quantities are defined as previously. When scattering is neglected, Gurevich *et al.* obtain a result equal to Eq. (8) with $v_z^0/s = 1$ (when the sound propagation is parallel to the magnetic field, $v_z^0 = s$). When $B \gg 1$, Gurevich *et al.* obtain the result

$$\Gamma_{\max}/\Gamma_{\min} \sim ql(\hbar\Omega/\zeta)^{1/2}(\hbar\Omega/kT) \gg 1. \tag{17}$$

[10] V. G. Skobov, Zh. Eksperim. i Teor. Fiz. **40**, 1446 (1961) [English transl.: Soviet Phys.—JETP **13**, 1014 (1961)].
[11] J. S. Dhillon and D. Shoenberg, Phil. Trans. **A248**, 1 (1955).

When $B \sim 1$,

$$\Gamma_{max}/\Gamma_{min} \sim (\hbar\Omega/kT)^{3/2}. \quad (18)$$

III. DISCUSSION OF EXPERIMENTAL TECHNIQUES

A. Method of Making Measurements

Because the technique for making the measurements to be presented is new, it will be discussed in some detail. The usual method for measuring attenuation coefficient is shown in Fig. 2(a). The pulsed oscillator produces an rf pulse of the proper frequency. At the transmitting transducer T_1, a fraction of this electrical energy is converted into a sound pulse of the same frequency which enters the sample S. The sound pulse travels across the sample undergoing attenuation characteristic of the sample. At the opposite face, a small fraction of the sound energy enters the "receiving" transducer and is converted into an electrical signal which is amplified, demodulated in the detector and displayed on the cathode-ray oscilloscope (CRO). Most of the sound energy incident on the sample surface at T_2 does not leave the sample, however, but is reflected. This energy travels back to the first surface, is again reflected and travels back to T_2 where again a small fraction of the incident sound energy is converted into an electrical pulse which is displayed on the CRO, thus producing a second pulse. This pulse, however, is smaller than the first pulse because of the attenuation suffered in traveling twice the sample thickness. As this process of reflections continues, the signal displayed on the CRO consists of a succession of pulses as shown in Fig. 3, an echo train derived from the initial sound pulse which entered the sample. Each pulse is delayed from its predecessor by the time for a round trip across the sample. The envelope of the pulses is an exponential characteristic of the acoustic attenuation in the sample. This attenuation is characterized by the attenuation coefficient, or the logarithmic decrement per unit length of sample traversed. The attenuation coefficient is defined by the equation for the pulse amplitude.

$$A = A_0 e^{-\Gamma d}, \quad (19)$$

where d is the distance traversed, Γ is the attenuation coefficient, and A_0 is the amplitude at $d=0$. If one photographs the CRO trace, he can calculate Γ from measurements of the echo train. If one wishes to vary some independent parameter X and measure $\Gamma(X)$, this can be done by taking successive photographs. However, if Γ is a rapidly varying function of X so that a large number of photographs is necessary, the procedure can become quite tedious and time consuming. The method is also rather unsuitable for measuring small changes in Γ. To overcome these difficulties, a sampling system becomes attractive. Here, one selects a particular pulse in the echo train and measures its amplitude as a function of X. Because of the exponential dependence of A upon Γ, this technique provides high sensitivity. There are, of course, many ways to measure the variation in pulse height. The simplest is merely to measure the height of a particular pulse on the face of the CRO. This is, of course, greatly facilitated by using large gain plus a dc offset voltage by means of which the peak of the pulse is kept in view. A more sophisticated scheme, which has been widely employed,[12] is the use of an electronic gating circuit to select a particular pulse which is then integrated. Thus, the output of the integrator will be proportional to the area under the pulse.

The scheme which we propose involves the use of a commercial sampling oscilloscope. This contains elaborate gating circuits with rectified outputs which can be used to actuate an x-y recorder. The circuits are very stable, allowing accurate locking on any desired point on the input signal, with a dc output proportional to the signal amplitude at this point. In addition, the sampling oscilloscopes have a high sensitivity, on the order of millivolts, and have a very wide bandwidth extending from dc to the kilomegacycle region. Thus, the sampling oscilloscope provides a very versatile tool. Its use is illustrated in Fig. 2(b). The output of the amplifier is fed to the sampling scope. From the sampling scope is obtained an output proportional to the signal amplitude at a specified point. This output then goes to the y (vertical) input of a recorder. To the x (horizontal) input of the recorder is sent a signal proportional to the independent variable X. For example, the independent variable might be magnetic field, electric field, angle, temperature, or time. If one

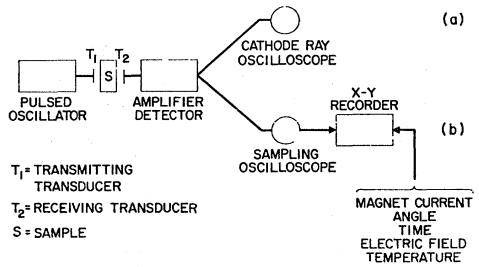

FIG. 2. Block diagram of the apparatus.

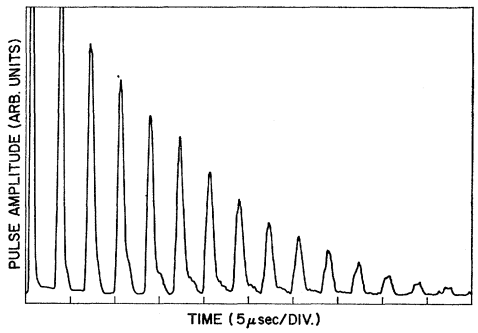

FIG. 3. Typical pulse echo train.

[12] G. N. Kamm and H. V. Bohm, Rev. Sci. Instr. 33, 957 (1962).

uses the internal sweep circuit of the sampling scope, one can trace out the input signal. This is, in fact, how Fig. 3 was obtained—the x input to the recorder coming from the horizontal output of the sampling scope, which provides a dc voltage proportional to the time swept out by the internal sweep circuit. The instrument used in this experiment was a Tektronix 661 sampling oscilloscope with a Type 5T1A Timing Unit and a Type 451 Dual Trace Sampling Unit. The other equipment used is as follows: an Arenburg PG-650C pulsed oscillator, Arenburg PA-620-SN211 preamplifier, Arenburg WA-600B amplifier, and a Moseley 135 recorder. The transducers were Y- or AC-cut quartz obtained from the Valpey crystal Corporation.

In the results to be discussed in this paper, it is the variation in attenuation coefficient with magnetic field under various conditions which is of interest. The magnetic field was supplied by a Bitter type iron core electromagnet, manufactured by Arthur D. Little, Inc. By means of a manual sweep control, the oscilloscope was synchronized on the peak of the desired echo of the reflection train. The y axis of the recorder was then driven by the vertical output of the oscilloscope, the x axis by a signal proportional to the magnet current. The results will be presented later.

B. Sample Preparation

The results to be presented were obtained from two bismuth samples which were cut using a spark cutter from single crystals that were oriented by the Laue x-ray back-reflection technique. Sample Bi 14 was cut from a crystal provided by Metals Research Ltd. which is supposed to be 99.999% pure. It was cut to a thickness of nearly one centimeter, and the opposite faces were mechanically lapped and polished flat and parallel. Sample LXI-F1 was cut from a crystal grown by the Czochralski method from a melt of 99.9999% pure bismuth. Its thickness was about 0.25 cm and its opposite faces were made flat and parallel by spark planing. Both samples suffered some surface damage as evidenced by x-ray diffraction photographs. The orientations of the two samples were nearly the same, i.e., with the parallel surfaces nearly perpendicular to the bisectrix direction. For sample LXI-F1, the surface normal was within 0.2° of bisectrix; for sample 14, the normal was tilted 1.8° toward the trigonal direction and 0.8° toward the binary direction. The transducers were bonded to Bi 14 with Eastman 910 adhesive, to LXI-F1 with GE 7031 varnish baked 12 h at 65°C.

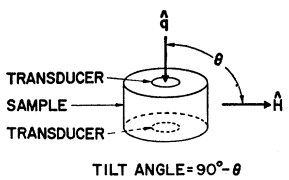

FIG. 4. Sample geometry.

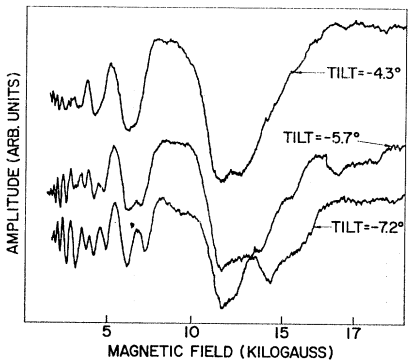

FIG. 5. Variation of transmitted acoustic pulse height as a function of applied magnetic field for tilt angles of −7.2°, −5.7°, and −4.3°, respectively. The length of sample traversed is about 0.5 cm, the frequency was 45 Mc/sec and the temperature was 1.8°K.

Both adhesives were found to be satisfactory, although there was some evidence that the 910 adhesive strained the sample somewhat more.

IV. EXPERIMENTAL RESULTS

Consider first the tilt effects. The geometry is shown in Fig. 4. The sound propagation direction, $\hat{q}$, is nearly perpendicular to the field direction $\hat{H}$, the angle between them designated as θ. We define a "tilt angle" as $90°-\theta$. The applied transverse acoustic waves are propagated in the bisectrix direction with their polarization in the binary direction. The magnetic field is approximately in the binary direction. The results for sample LXI-F1 at a frequency of 45 Mc/sec and a temperature of 1.8°K are shown in sequence in Figs. 5, 6, and 7. The oscilloscope is synchronized on a pulse which has traversed two sample thicknesses, i.e., 0.5 cm of bismuth. The traces shown are pulse amplitude versus applied magnetic field for various tilt angles, from −7.2° to +5.7°. As one can see, the amplitude of the oscillations reaches a maximum at about −2.9°, decreases to zero at about 0°, then passes through another maximum at approxi-

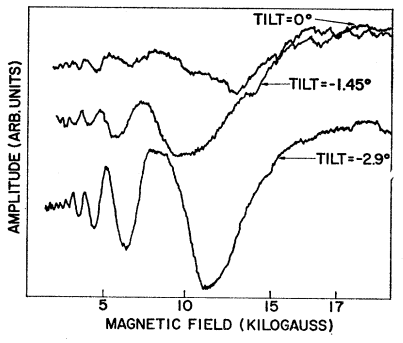

FIG. 6. Variation of transmitted acoustic pulse height as a function of applied magnetic field for tilt angles of −2.9°, −1.45°, and 0°, respectively. The length of sample traversed is about 0.5 cm, the frequency was 45 Mc/sec and the temperature was 1.8°K.

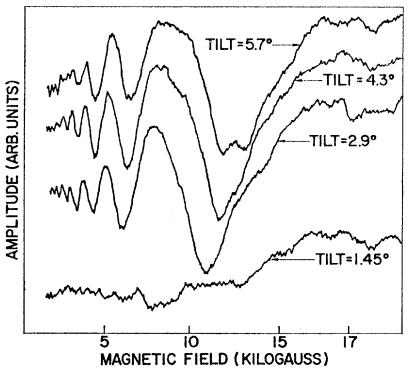

FIG. 7. Variation of transmitted acoustic pulse height as a function of applied magnetic field for tilt angles of +1.45°, +2.90°, +4.3°, and +5.7°, respectively. The length of sample traversed was about 0.5 cm, the frequency was 45 Mc/sec and the temperature was 1.8°K.

mately +2.9°. Thus, we see that the results are nearly symmetric about zero (which occurs at an indicated angle of about +0.7°), with maxima in the amplitude at ±3° and a minimum at 0°.

The second set of results is concerned with the change in amplitude of the giant oscillations with the quantity ql. A very simple way to vary ql is by varying the frequency of the sound. This was done by operating on the odd harmonics of the transducers. Thus, in Figs. 8–10 are shown plots of amplitude versus magnetic field for sample 14 taken under identical experimental conditions except that the frequencies were 8, 26, and 43 Mc/sec, respectively. Hence, the values for ql are approximately in the ratio 1:3:5. The amplifier gain was adjusted so that at each frequency the signal amplitude in zero field was about the same. It is clear that the amplitude of the oscillations increases monotonically with ql. The experimental conditions for Figs. 8–10 are the following: tilt angle $\simeq 2°$, $\hat{H}$ in the binary direction, $\hat{q}$ in the bisectrix direction, polarization in the binary direction, and the temperature was about 1.5°K. The pulse studied was one which had traversed one sample thickness, i.e., about one centimeter.

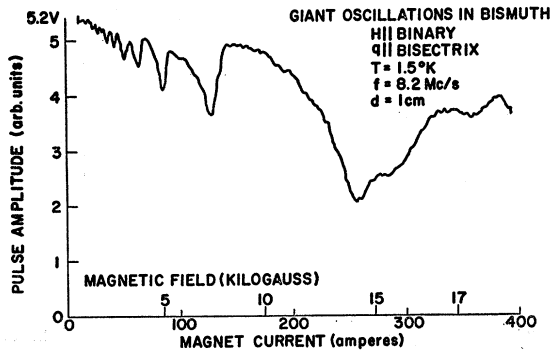

FIG. 8. Variation of acoustic pulse height as a function of applied magnetic field at a frequency of 8.2 Mc/sec for a sample length of 1 cm and a tilt angle of 2°.

V. DISCUSSION OF RESULTS

In discussing the comparison between experiment and theory, there are two levels at which the data should be examined. First, there is the qualitative aspect: Do the results show the broad features predicted by the theory? Secondly, there is the quantitative aspect: Do the results agree in detail with the theory?

Firstly, let us consider the amplitude of the quantum oscillations of attenuation coefficient. As the results of Skobov suggest, i.e., Eq. (13), the oscillations grow in amplitude with increasing magnetic field, only becoming large at fields greater than ~3000 Oe. Thus Reneker,[1] who measured ultrasonic attenuation in bismuth up to 1600 Oe, never attained this region in which the giant oscillations would have been visible. At 40 Mc/sec, changes in attenuation coefficient as large as 2 cm^{-1} were observed in both of the samples discussed in this paper. Accurate measurements of Γ_0, the attenuation coefficient in zero magnetic field, have not been

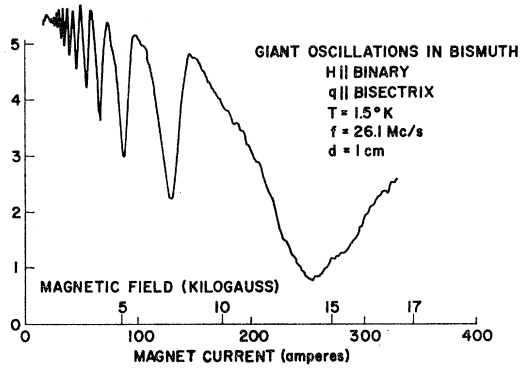

FIG. 9. Variation of acoustic pulse height as a function of applied magnetic field at a frequency of 26.1 Mc/sec for a sample length of 1 cm and a tilt angle of 2°.

carried out yet at 40 Mc/sec, but it is estimated to be about 1 cm^{-1} for Bi 14. Thus, $\Gamma_{max}/\Gamma_0 \approx 2$. This is quite a sizable effect. For a path length of one centimeter, a change in attenuation coefficient of 2 cm^{-1} indicates a change in pulse height by a factor of 7. However, from Eq. (10), we calculate $\Gamma_{max}/\Gamma_0 \sim 10^3$ at 14 000 G. Likewise, from Eq. (11) we calculate $\Gamma_{min}/\Gamma_0 \sim 10^{-37}$ at 8600 G, whereas we observe $\Gamma_{min}/\Gamma_0 \approx 1$.

Next, let us examine the variation of Γ_{max} with magnetic field. From Eq. (10), it is apparent that Γ_{max} should vary linearly with magnetic field. The maxima in attenuation coefficient will, of course, correspond to minima in the amplitude of the acoustic pulse. In Fig. 11, we have plotted the logarithm of the amplitude minima versus the magnetic field at which the minima occur for the data of Figs. 8 and 9, i.e., 8 and 26 Mc/sec, respectively. It is clear that the data fall, within experimental error, on a straight line, as one would expect from Eq. (10). The data at 40 Mc/sec, which are not plotted, also lie approximately on a straight line. Thus,

again we get qualitative agreement with Eq. (10). However, the magnitude of the slope is incorrect by two orders of magnitude. The measured slope at 8 Mc/sec is 0.026 $(kG)^{-1}$. The slope calculated from Eq. (10), taking $\Gamma_0(8\text{ Mc/sec}) \approx 0.2\text{ cm}^{-1}$ and $v_z^0/s \approx 25$, is 14 $(kG)^{-1}$, a factor of 500 larger. In the case of Γ_{min}, there does not seem to be even qualitative agreement between theory and experiment. To check the effect upon the giant oscillations of variation of ql, $\Gamma_{max}/\Gamma_{min}$ was calculated for frequencies of 8, 26, and 43 Mc/sec from the data of Figs. 8–10 at $H = 7500$ G. It was found that $\Gamma_{max}/\Gamma_{min}$ was about two at each frequency, and was thus independent of ql. The latter is in agreement with the prediction from Eqs. (10) and (11) or (16), but again the numerical value of the ratio is far smaller than that predicted from the theoretical models.

Next, consider the angular dependence of the giant oscillations. As Figs. 5, 6, and 7 indicate, the oscillations

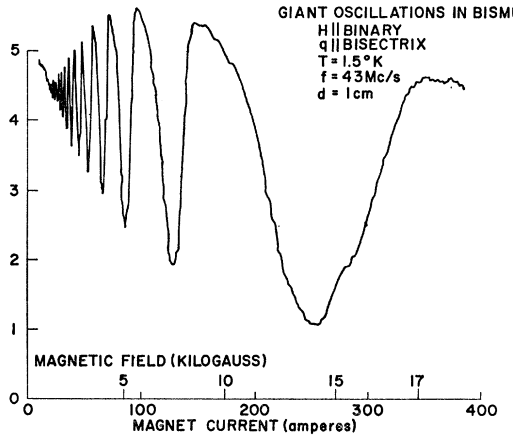

FIG. 10. Variation of acoustic pulse height as a function of applied magnetic field at a frequency of 43 Mc/sec, a tilt angle of 2° and a sample length of 1 cm.

are largest at tilt angles of nearly 0° and become very small at exactly 0°. These results are in qualitative agreement with the theoretical predictions of Sec. II. However, from Eqs. (8) and (9) one would expect the maxima in the oscillations to occur at tilt angles such that $k_z^0 \approx k_F$ or $\cos\theta \approx 10^{-3}$. The tilt angle at which the oscillations were actually observed to be a maximum was about fifty times larger than this estimate. In addition, sample Bi 14 showed only a relatively small tilt effect with the oscillations not vanishing for any angle.

In considering the results discussed so far, which have all been concerned with the magnitude of the giant oscillations, it is clear that the experimental results demonstrate qualitatively the features predicted by the theoretical model. However, the magnitude of the observed effects is not in agreement with what one would expect from the theoretical model. There are at least two causes for these discrepancies. There is first of all

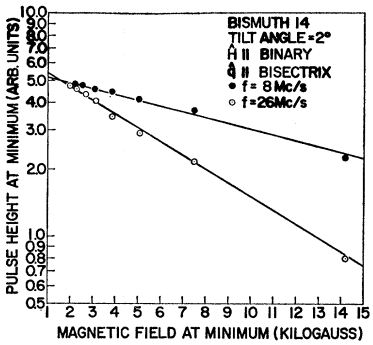

FIG. 11. Magnetic field dependence of pulse-height minima. The data are from Figs. 8 and 9.

the problem of properly taking into account the magnitude of ql for the carriers giving rise to the observed oscillations of attenuation coefficient. Secondly, there is the problem of subtracting the attenuation of those carriers not involved in the oscillatory phenomena. For bismuth with the magnetic field in the binary direction, there are two groups of electrons and one group of holes[13] with cyclotron masses of $0.01m_0$, $0.1m_0$, and $0.2m_0$, respectively. As we show below, the observed quantum oscillations have a period characteristic of the lightest of these carriers. Thus, while the variations in attenuation coefficient with magnetic field can be largely attributed to the carrier of cyclotron mass $0.01m_0$, the background attenuation will contain contributions from the other two groups of carriers.

Furthermore, there is the possibility that not all of the observed ultrasonic absorption is electronic. Experimentally, Γ_{max} and Γ_{min} are measured relative to Γ_0, the attenuation in zero magnetic field. However, if the measured attenuation coefficient in zero field is not entirely electronic, the derived values of Γ_{max} and, particularly, Γ_{min} will be in error. The disagreement in the angular dependence of the oscillations is probably the effect of finite ql. Evidence for this can be found in the calculations by Spector.[14] Spector has considered in some detail the angular dependence of the nonoscillatory part of the magnetoacoustic attenuation on the basis of a two spherical band model. He finds that the tilt angle at which the attenuation maximum occurs, and indeed the sharpness of the maximum, depend strongly on $\omega\tau$ (or ql). In fact, from Fig. 1 or 2 of Spector's paper, which was plotted using parameters appropriate for bismuth, one would estimate that for sample LX*I*-F1, $\omega\tau \sim 0.1$ or $ql \sim 400$ at 40 Mc/sec.

Let us consider next the periodicity of the oscillations. We note in passing that only one period is observed, i.e., only one carrier contributes significantly to the quantum oscillations. In Fig. 12 is plotted the reciprocal of the magnetic field at each observed minimum in amplitude versus the index of the minimum, for the

[13] Yi-Han Kao, Phys. Rev. **129**, 1122 (1963).
[14] Harold N. Spector, Phys. Rev. **120**, 1261 (1960).

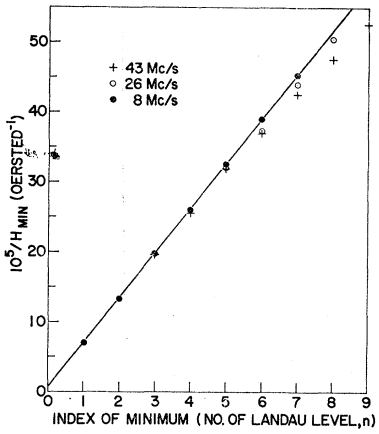

FIG. 12. Periodicity in the reciprocal of magnetic field for the pulse-height minima of Figs. 8, 9, and 10.

data of Figs. 8–10, i.e., at 8, 26, and 43 Mc/sec, respectively. The data obtained at 8 Mc/sec lie quite well on a straight line of slope 6.3×10^{-5} Oe^{-1}. This slope is about 8% lower than that measured by Reneker, who obtained 6.8×10^{-5} Oe^{-1} in magnetoacoustic measurements at 12 Mc/sec for magnetic fields below 1600 Oe. From Eq. (12), one calculates a slope of 6.12×10^{-5} Oe^{-1} taking for m_c the value $0.0107m_0$ measured by Kao[13] for the lightest carriers in this direction, and for ζ the value 0.0177 eV obtained by Dhillon and Shoenberg.[11] The data taken at 43 Mc/sec coincide with the 8 Mc/sec data at the higher magnetic fields, i.e., $H>5000$ Oe, but appear to deviate at the lower magnetic fields. The 26 Mc/sec data fall between the 8 and 43 Mc/sec data. The reason for this departure from periodicity at the higher frequencies is not understood. One can speculate, however. Were electronic transitions with $\Delta n=1$ to occur [see Eq. (3)], one would expect deviation from periodicity in $1/H$. This point is discussed by Gantsevich and Gurevich,[15] who obtain for the period of the oscillations the expression:

$$\Delta\left(\frac{1}{H}\right)=\frac{2\pi e\hbar}{cS}\left[1+\frac{2\pi e\hbar l k_z}{cSq_z g'(k_z)}H\right]^{-1}, \tag{20}$$

where

$$\Delta n=l, \tag{21}$$

and where S is the cross-sectional area of the Fermi surface in momentum space.

The quantity $g'(k_z)$ depends upon the topology of the Fermi surface, but for a free electron model, it is -1. Thus, we see that for $\Delta n\neq0$, the oscillations are not strictly periodic, i.e., the period is a slowly varying function of magnetic field. Let us now consider the conditions under which transitions of the type $l\neq0$ can occur. From Eq. (3), we see that such transitions can only occur for those carriers for which

$$k_z=k_z{}^0=\frac{m^*l\Omega}{\hbar q_z}=\frac{m^*}{m_c}\frac{leH}{c\hbar q_z}, \tag{22}$$

since $\omega\ll\Omega$ for the magnetic field values and sound frequencies with which we are concerned. We can also rewrite Eq. (22) in terms of the carrier velocity to correspond to Eq. (6).

$$v_z{}^0=(l\Omega/\omega)(u/\cos\theta). \tag{23}$$

Since the maximum allowable value for $v_z{}^0$ is v_F, the Fermi velocity, the $l\neq0$ transitions can only occur for magnetic fields below a critical value determined from Eq. (23) or (22) which depend upon the phonon frequency, etc. For the experimental results shown in Fig. 10, i.e., $f=40$ Mc/sec, $\hat{q}=$ bisectrix, and $\hat{H}=$ binary, $v_z{}^0$ at $l=1$ is equal to 6×10^{10} cm/sec for $H=2000$ G and is even greater for larger magnetic fields. Therefore, $v_z{}^0(l=1)/v_F\gtrsim10^3$, and this transition is thus impossible. What then is the explanation of the deviations from periodicity in $1/H$? In the simple theory of Sec. II, upon which the results have been interpreted thus far, the energy bands have been assumed to be parabolic, i.e., quadratic in the momentum. However, recent theoretical and experimental work[16–18,13] indicates that the bands may be quite nonparabolic, so that the cyclotron mass is energy dependent, or equivalently, field-dependent. The expression derived by Lax *et al.*,[17] assuming two sets of interacting energy bands near the band edge is the following:

$$\epsilon=-\frac{\epsilon_G}{2}\pm\left\{\left(\frac{\epsilon_G}{2}\right)^2+\epsilon_G\left[(n+\tfrac{1}{2})\hbar\Omega+\frac{\hbar^2k_z^2}{2m^*}\pm\frac{\beta}{2}g_{\rm eff}H\right]\right\}^{1/2}. \tag{24}$$

In the above expression ϵ_G is the energy gap, β is the Bohr magneton, and $g_{\rm eff}$ is the spectroscopic splitting factor, which gives rise to spin splitting of the levels. The plus and minus signs in front of the curly bracket refer to the conduction and valence bands, respectively. It is clear that the energy level spacing and curvature of the model of Eq. (24) are quite different from those of Eq. (1). Hence, one would not be too surprised to see deviations from periodicity if Eq. (24) is a correct description. This point will be investigated and reported in a future communication.

Still another feature of the giant oscillations is the asymmetry of the minima in pulse height as shown in Figs. 8–10. This feature is more pronounced, perhaps, in Fig. 13, which shows another interesting feature, spin

[15] S. V. Gantsevich and V. L. Gurevich, Zh. Eksperim. i Teor. Fiz. **45**, 587 (1963) [English transl.: Soviet Phys.—JETP **18**, 403 (1964)].

[16] B. Lax, Bull. Am. Phys. Soc. **5**, 167 (1960).

[17] B. Lax, J. G. Mavroides, H. J. Zeiger, and R. J. Keyes, Phys. Rev. Letters **5**, 241 (1960).

[18] M. H. Cohen, Phys. Rev. **121**, 387 (1961).

splitting, which is clearly resolved in the minimum occurring at 15 000 Oe, but is not resolved in the minima occurring at lower magnetic fields. This spin splitting has also been observed in quantum oscillations of the temperature[19] and magnetoresistance[20] of bismuth. In Fig. 14 is shown a plot of pulse amplitude versus magnetic field, as calculated from Eq. (8), which neglects electron scattering. Not only are the experimental minima broader than those of the theoretical model, but they have a characteristic gentle slope on the low field side, a much steeper slope on the high field side. While the model of Gurevich *et al.*[5] would predict broadening if electronic scattering were important, the broadening which it predicts would be symmetric. Unresolved spin splitting would also cause broadening, but again, this should be symmetric. In a previous communication,[8] we suggested that this unsymmetric broadening was caused by electronic scattering, in contradiction to the model of Gurevich *et al.* Preliminary calculations by Liu[21] for a model of the giant oscillations which includes collision broadening indicates that this explanation is correct. These calculations will be published in the near future.

VI. SUMMARY OF RESULTS

As we have suggested throughout this paper, the results must be examined at two levels—the qualitative and the quantitative.

Qualitatively, the data bear out many of the features of the theoretical models at high magnetic fields. One sees very large quantum oscillations of the magnetoacoustic attenuation. Changes as large as 17 dB/cm have thus far been observed. The oscillations are approximately periodic in the reciprocal of the magnetic field, the period corresponding to the lightest cyclotron mass. The maxima in attenuation coefficient increase linearly with magnetic field, as the theory predicts. In addition, in one of the two samples, the predicted angular dependence of the oscillation amplitude was observed. Quantitatively, the experiments are in poor agreement with the theoretical predictions, differing in some instances by orders of magnitude. For example, the observed maxima in attenuation are not nearly so large as the simple theory predicts; the observed minima not nearly so small. Although one sample showed an angular variation of the amplitude of the quantum oscillations, the other showed little or no angular variation. Furthermore, although the oscillations at 8 Mc/sec were periodic in the reciprocal of the magnetic field, those at 42 Mc/sec exhibited deviations from periodicity which are estimated to be outside of experimental error. In addition, there are two experimental features not at all predicted by the theoretical models. There is the asymmetry of the minima in transmitted pulse height (or maxima in attenuation coefficient) and there is the enhanced spin splitting in the pulse height minimum occurring at 15 000 Oe.

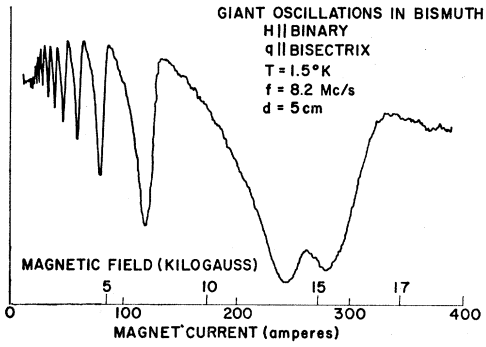

FIG. 13. Variation of acoustic pulse height as a function of applied magnetic field at a frequency of 8.2 Mc/sec, a tilt angle of 2°, and a sample length of 5 cm.

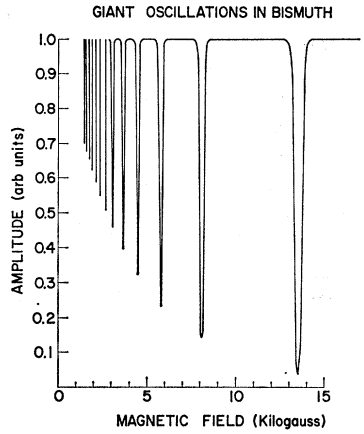

FIG. 14. Variation of acoustic pulse height as a function of applied magnetic field at a temperature of 1.5°K as calculated from the theoretical model of Kazarinov and Skobov. The calculations, which neglect spin splitting, are from Eq. (8) for the following values of the parameters: $\Gamma_0=0.0024$ cm^{-1}, $d=1$ cm, $C=e\hbar/m_e c=1.08\times10^{-6}$ eV/G, $kT=1.29\times10^{-4}$ eV, and $\zeta=0.022$ eV.

It is felt that most, if not all, of the discrepancies noted above would be resolved by a more sophisticated model which would include the important features not taken account of by the model of Kazarinov and Skobov[9]—electronic scattering by defects, effects of more than one type of carrier, and deviations from parabolicity of the conduction bands in bismuth. Indeed, preliminary calculations by Liu[21] which include the effects of defect scattering of electrons upon the giant oscillations indicate that inclusion of this feature will explain the discrepancies in the amplitude of the quantum oscillations as well as the asymmetry of the minima in transmitted pulse height. However, it does not appear to explain the deviation from periodicity. The latter may be a consequence of the nonparabolicity of the energy bands and will be investigated further.

[19] W. S. Boyle, F. S. L. Hsu, and J. E. Kunzler, Phys. Rev. Letters 4, 278 (1960).
[20] Lawrence S. Lerner, Phys. Rev. **130**, 605 (1963).
[21] S. H. Liu (private communication).

Finally, we should like to point out the versatility of the scheme suggested in Sec. IIIA for making measurements of ultrasonic attenuation. This method, which utilizes a commercial sampling oscilloscope together with an X-Y recorder, enables one to record the data directly onto a sheet of graph paper. As Fig. 3 illustrates, one can record the pulse echo train directly by using the internal sweep of the oscilloscope. To measure the variation of attenuation coefficient with some independent variable, one may select any echo in the echo train and measure its change in amplitude as the independent variable is changed in magnitude. This technique is illustrated in Figs. 5–10 and 13, in which the variation of pulse amplitude with applied magnetic field under various circumstances has been recorded.

ACKNOWLEDGMENTS

The authors would like to express their appreciation to Dr. P. B. Miller and Dr. S. H. Liu for many informative discussions, and to Dr. P. E. Seiden for many helpful suggestions concerning the manuscript, and to R. E. Mundie for his assistance in preparing the samples and carrying out the measurements.

PHYSICAL REVIEW VOLUME 137, NUMBER 1A 4 JANUARY 1965

Electronic Specific Heat and Saturation Magnetization of Cr-Fe and Fe-Co Alloys*

L. BERGER
Carnegie Institute of Technology, Pittsburgh, Pennsylvania
(Received 17 July 1964; revised manuscript received 26 August 1964)

The collective model of ferromagnetism is applied to various models for the upper third of the $3d$ band profile of bcc alloys of transition metals. In the first band profile, we consider a rectangular sub-band with rounded lower and upper edges, assuming an intra-atomic exchange integral just large enough to produce ferromagnetism. The low-temperature specific-heat coefficient γ is found to have a sharp peak at the electron concentration where ferromagnetism starts (almost empty sub-band) and a deep minimum at the concentration with largest saturation magnetization (half-filled sub-band). This agrees qualitatively with the measurements by Cheng, Wei, and Beck in Cr-Fe and Fe-Co alloys. The agreement becomes quantitative if a second similar model of the band profile is used where the density of states inside the sub-band is not constant, but drops linearly with increasing energy. The calculated zero-temperature saturation magnetizations agree well with the Slater-Pauling curve for these alloys. In a third model, the sharp peak of γ is not a simple consequence of the action of the collective model, but reflects the existence of a real peak in the assumed band profile. Then this peak of γ is predicted to happen at an electron concentration slightly larger than the one at which ferromagnetism starts; this seems to be found experimentally in the Cr-Fe series. The calculated saturation magnetizations again agree with the Slater-Pauling curve.

INTRODUCTION

A GREAT wealth of experimental data on the electronic specific heat of body-centered cubic alloys of the first transition series is now available, due to the work of Cheng, Wei, and Beck[1] and of other authors.[2–6] This gives direct information about the profile of the $3d$ band, at least in the case of alloys where no ferromagnetic spin polarization is present.

The purpose of the present work is to investigate theoretically the effect of a ferromagnetic spin polarization on the low-temperature electronic specific heat of bcc alloys in the framework of the collective approach to ferromagnetism, assuming various models of the band profile. Using the same models, the zero-temperature saturation magnetizations for these series of alloys have also been computed, to be compared with the well-known experimental Slater-Pauling curve.[7–13] The present work should also provide a general picture of the electronic structure of the ferromagnetic bcc iron alloys.

It is by comparing the predictions of the collective model with the magnetization data that Slater[7] and Pauling[8] were able to conclude that a region of low density of states should exist in the profile near the Fermi level of chromium. Unfortunately, the value of the magnetization is rather insensitive to the details of

* Work supported in part by the U. S. Office of Naval Research and the National Science Foundation.

[1] C. H. Cheng, C. T. Wei, and P. A. Beck, Phys. Rev. **120**, 426 (1960).
[2] K. Schröder, Phys. Rev. **125**, 1209 (1962).
[3] E. A. Starke, C. H. Cheng, and P. A. Beck, Phys. Rev. **126**, 1746 (1962).
[4] K. Schröder, Phys. Rev. **117**, 1500 (1960).
[5] K. Schröder and C. H. Cheng, J. Appl. Phys. **31**, 2154 (1960).
[6] K. Schröder, J. Appl. Phys. **32**, 880 (1961).
[7] J. C. Slater, Phys. Rev. **49**, 537, 931 (1936).
[8] L. Pauling, Phys. Rev. **54**, 899 (1938).
[9] W. Shockley, Bell System Tech. J. **18**, 645 (1939).
[10] P. Weiss and R. Forrer, Ann. Phys. **12**, 279 (1929).
[11] M. Fallot, Ann. Phys. **6**, 305 (1936).
[12] A. Arrott and H. Sato, Bull. Am. Phys. Soc. **3**, 42 (1958).
[13] M. V. Nevitt and A. T. Aldred, J. Appl. Phys. **34**, 463 (1963).